INT. J. REMOTE SENSING, 1995, VOL. 16, NO. 17, 3459–3479

Analysis of coastal ice cover using ERS-1 SAR data

G. LESHKEVICH

NOAA/Great Lakes Environmental Research Laboratory, 2205 Commonwealth Boulevard, Ann Arbor, Michigan 48105-1593, U.S.A.

W. PICHEL, P. CLEMENTE-COLON, R. CAREY

NOAA/NESDIS/Satellite Research Laboratory, 5200 Auth Road, Camp Springs, Maryland 20746–4304, U.S.A.

and G. HUFFORD

NOAA/National Weather Service, 222 W. 7th Avenue, Anchorage, Alaska 99513–7575, U.S.A.

Abstract. An applications demonstration of the use of Synthetic Aperture Radar (SAR) data in an operational setting is being conducted by the National Oceanic and Atmospheric Administration (NOAA) CoastWatch Program. In the development phase of this demonstration, case studies were conducted to assess the utility of SAR data for monitoring coastal ice in the Bering Sea, icebergs from calving glaciers in Prince William Sound, and lake ice in the Great Lakes. ERS-1 SAR data was used in these studies. Results showed that depending on size and sea state icebergs could be detected from background and computer enhanced in the imagery, that SAR data can supplement and enhance the utility of satellite visible and infrared data sources for coastal ice monitoring, and that Great Lakes ice cover can be classified by ice type and mapped in the SAR data using image processing techniques. Cloud cover was a common problem. Based on the further development of automated analysis algorithms and the increase in frequency of SAR coverage, the all-weather, day/night viewing capabilities of SAR make it a unique and valuable tool for operational ice detection and monitoring.

1. Introduction

The launch of the First European Remote-Sensing Satellite (ERS-1) in July 1991, marked the beginning of a wealth of satellite-borne Synthetic Aperture Radar (SAR) data which will be available in the 1990s. In order to develop expertise in SAR applications and the capability to handle SAR data in an operational setting, an applications demonstration of the use of ERS-1 data for coastal environmental systems management is being carried out within the CoastWatch theme of the National Oceanic and Atmospheric Administration (NOAA) Coastal Ocean Program. This applications demonstration has focused on coastal ice analysis for navigation and hazard warning in Alaska and the Great Lakes; however, other management applications such as analysis of ocean current and eddy features for fisheries management, and monitoring of river ice jams for flood warnings have also been studied. The development phase of the applications demonstration began in July 1992, with the actual demonstrations taking place in 1994. The ice applications studied in the development phase are the subject of this paper.

2. CoastWatch

2.1. *CoastWatch goal and organization*

CoastWatch is a theme program within NOAA's Coastal Ocean Program. The goal of CoastWatch is to provide data and products for near real-time monitoring of U.S. coastal waters in support of environmental science, management, and hazard warning. Satellite data mapped for CoastWatch by the National Environmental Satellite, Data, and Information Service (NESDIS) along with *in situ* and weather-model data covering the entire U.S. coastal zone are now being distributed electronically via the NOAA Ocean Products Centre (OPC), eight NOAA field offices or CoastWatch Regional Sites (CRSs), and the NOAA National Oceanographic Data Centre (NODC). Current CoastWatch satellite products include satellite sea surface temperature (SST) and visible/near-infrared images (used for cloud and turbidity mapping) at 1·1–1·3 km resolution derived from the Advanced Very High Resolution Radiometers (AVHRR) carried on the NOAA polar-orbiting satellites (Pichel *et al.* 1991). CoastWatch products are used for environmental monitoring of coastal ocean conditions such as; (1) location and concentration of ice which may affect safety of coastal transportation as well as oil industry and fishing activities, (2) position of eddies and current/water-mass boundaries which may affect fishery studies or research vessel sampling strategies, and (3) temperature of the water which may influence the distribution of endangered turtle species, the optimal conditions for release of hatchery fish, and the spread and growth of Zebra Mussels.

Planned for the near future are ocean-colour products from the Sea-viewing Wide Field-of-view Sensor (SeaWiFS) instrument on the SeaStar satellite, lake and ocean model output from the Great Lakes Forecasting System and planned NOAA Coastal Forecast System, ocean surface wind speed data from the Defense Meteorological Satellite Program (DMSP) Special Sensor Microwave/Imager (SSM/I) and SAR images and derived products from RADARSAT. For additional information on the NOAA CoastWatch Program see Celone and Smith (1992), Leshkevich *et al.* (1993).

3. CoastWatch SAR applications demonstration

3.1. *General description and goals*

The CoastWatch SAR Applications Demonstration has the goal of assessing the utility of SAR imagery for CoastWatch purposes. During the development phase of the applications demonstration (beginning June 1992), a limited number of coastal applications case studies were carried out to develop the capability to access, display, and analyse ERS-1 data. An applications demonstration was then conducted beginning January 1994, using the SAR data routinely in the Great Lakes, in support of ice reconnaissance and analysis. The ultimate goal of these activities is to prepare for operational use of SAR data in the latter half of the decade. Two CRSs are participating in the applications development and demonstration: (1) the National Weather Service (NWS) Anchorage Forecast Office (the CRS for Alaska), and (2) the Great Lakes Environmental Research Laboratory (GLERL) in Ann Arbor, Michigan (the CRS for the Great Lakes). For additional information on the CoastWatch SAR Applications Demonstration see Pichel *et al.* (1994).

3.2. *SAR coastal ice applications*

Lewis *et al.* (1987), describes the results of numerous studies to detect and classify sea-ice and icebergs, many of them using shore or ship-borne *X*-band (3 cm)

or *S*-band (10 cm) radars. The results of many of these studies point out that detection and classification of ice are dependent on the interaction of the physical characteristics of the ice, radar parameters, sea state, and platform (look angle). Hall and Martinec (1985), point out that the surface parameters found to influence the radar return signal are surface roughness, orientation, slope, and the complex dielectric constant. The dielectric constant for saline first-year ice is highly dependent on temperature, salinity, and brine volume but relatively independent of frequency above about 1 MHz. However, the dielectric loss for sea-ice is strongly dependent on frequency and temperature. The difference between the dielectric constant and the dielectric loss, or the relative complex permittivity is described by Lewis *et al.* (1987) as being the electrical property of sea-ice most important in the radar sensing of ice. In addition, the instrument parameters which also affect the intensity of the return signal are incidence angle, polarization, and frequency.

The SAR instrument aboard ERS-1 is a C-Band (5·66 cm) vertically polarized (send and receive) radar. The satellite is in sun synchronous orbit at an altitude of 785 km. The repeat cycle can vary among 3, 35, or 176 days. The incidence angles span 19·35 to 26·50° (23° at mid-range). The swath width is 100 km and maximum image resolution is 12·5 by 12·5 m. For additional instrument, system, orbit, and image information see Olmsted (1993) and Battrick (1993).

CoastWatch ice applications being studied with ERS-1 SAR data include (1) monitoring ice condition for coastal ocean and lake transportation including ice jams in straits, connecting channels, bays, and harbours, (2) monitoring icebergs resulting from glacial breakup, (3) monitoring ice hazards to oil activities, and (4) monitoring river ice jams and resultant flooding. As examples of these studies and as illustrations of the potential use of SAR in CoastWatch activities, the results of case studies in the first two applications, examining the interaction of ice and instrument parameters as illustrated in the imagery, are described in the following sections of this paper.

4. Coastal ice case studies in Alaska

The state of Alaska has approximately 54 per cent of the nation's coastline, and about 78 per cent of the state's population lives on or near the coast, usually located near a large river. Coastal and river transportation of goods is the major means of supply to these communities (less than 1 per cent of Alaska has roads). These waters are typically ice covered from November to May (all year for the Northslope waters). This ice becomes not only a hindrance to vessel traffic, but presents the potential for flooding due to river ice jams, especially in the spring. The NWS Anchorage Forecast Office maintains a sea-ice analysis and forecast programme for the coastal and offshore waters of Alaska. During the ice season, a sea-ice analysis is generated three times per week and includes a 5-day forecast for ice distribution and concentration.

4.1. *Forecasting of sea-ice in Bering Strait*

For ice analysis, the NWS Anchorage Forecast Office uses predominantly Advanced Very High Resolution Radiometer (AVHRR) imagery from the NOAA polar orbiting satellites. The AVHRR imagery provides a regional 'view' of the ice covered waters around Alaska. Because of the high latitude location of the Alaska region, over 14 passes are collected real-time each day from the two operational NOAA polar satellites. In the winter, with its short daylight period, infrared (IR)

imagery (1·1 km resolution at nadir) is the primary data used; however, its utility is hampered by cloudy weather. For very high resolution analysis and forecasting of ice, SAR data have proven to be a valuable supplement to AVHRR data.

A request was received in late February, 1994 concerning the state of ice conditions around the Diomede Islands in the Bering Strait (figure 1(*a*)). There was a need to be able to traverse the sea-ice in the Bering Strait near the islands. Figure 1 (*b*) shows the AVHRR IR image of the Bering Sea and Strait on 28 February 1994. Large leads are apparent both west and east of the Diomede Islands in the Strait. There is an indication of a polynya south of the islands. There also appears to be different ice along the Russian coast. An analysis of their thermal signatures (which average $-2°$ C to $-3°$ C) suggests that these lead and polynya features contain thin ice and new ice. A SAR image taken on the same day (figure 1 (*c*)) with the Diomede Islands visible in the image, clearly shows the shorefast (dark region along the Russian coast) and thin ice (striated, lighter-grey region seaward of the shorefast ice) off the Russian coast. The polynya (light-grey, striated region) is a prominent feature with its boundaries easily determined between the Diomedes, and extending south for over 30 km. There is also a narrow lead that extends north from the polynya between the Islands. It is evident from this SAR image that any effort to cross the ice between or south of the Islands could be, at the least, difficult.

Combined SAR and AVHRR imagery were also collected for 3 and 15 March 1994 (figures 1 (*d*)–(*f*)). The AVHRR image for 3 March is not included because of cloud cover over much of the Strait. The 15 March AVHRR image (figure 1 (*e*)) also has cloud cover over the western portion of the Strait; however, the Diomedes are evident in the imagery. The SAR image for 3 March (figure 1 (*d*)) shows a major decrease in the width and length of the polynya between, and south, of the Diomedes. Ice concentration around the Islands had become more consolidated. Based on this imagery, an effort was made to cross the ice. However, mechanical problems caused a postponement. The 15 March SAR image (figure 1 (*f*)) shows a dramatic change in sea-ice conditions. The polynya south of the Islands has increased in sea-ice cover. This consolidation in sea-ice is in response to a wind shift from northerly to southerly winds. A polynya can now be seen north of the Diomedes. Again, based on the imagery, the party was notified that ice conditions were favourable for an east–west crossing. Again mechanical problems haunted the group and the effort was abandoned. However, this exercise in using both SAR and AVHRR imagery to issue timely and detailed sea-ice forecasts proved to be highly successful.

4.2. *Monitoring icebergs in Columbia Bay*

Figure 2 illustrates the potential of SAR data as an aid in monitoring glacial breakup and iceberg hazards to shipping. On 24 March 1989, the oil tanker *Exxon Valdez* struck Bligh Reef (figure 2 (*a*)) when southbound out of Valdez, Alaska, the southern terminus of the Alaska pipeline. Eleven million gallons of oil fouled the pristine waters and shoreline of Prince William Sound. One of the contributing factors to the accident was the presence of ice in the shipping lanes. The *Exxon Valdez* deviated from the normal shipping lanes to avoid icebergs originating from the Columbia Glacier. One of the largest tidewater glaciers in Alaska, the Columbia Glacier is currently in retreat, often shedding large quantities of ice into Columbia Bay. These icebergs can be seen clearly on the 20 m resolution SPOT image in figure 2 (*b*). The location of the SPOT image is shown by the rectangle in figure 2 (*a*).

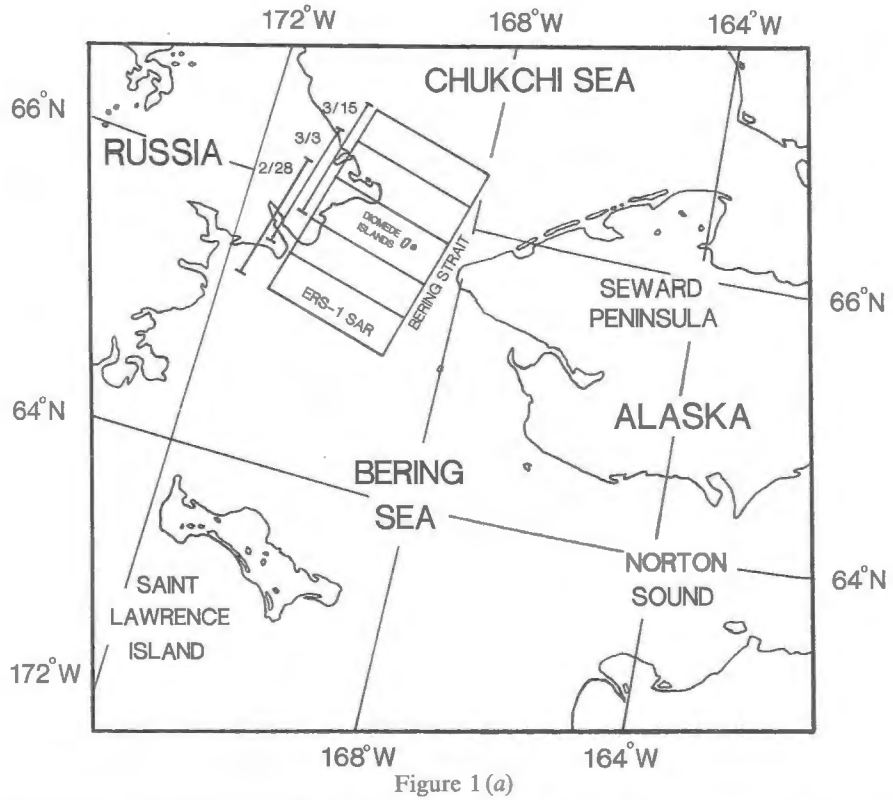

Figure 1 (*a*)

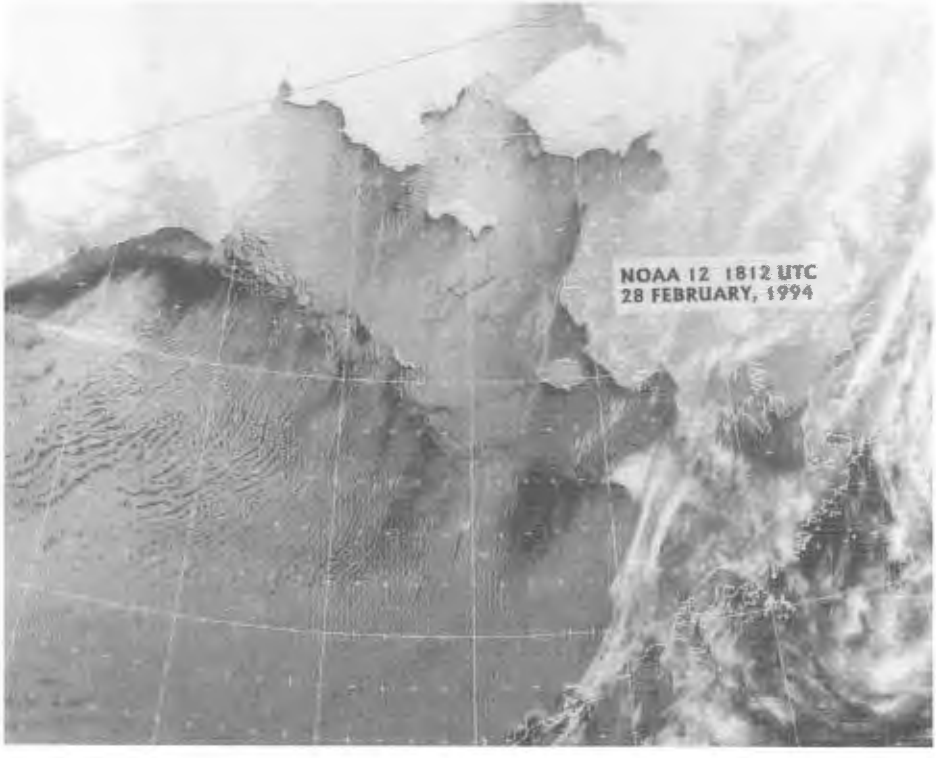

Figure 1 (*b*)

(*c*)

(*d*)

Figure 1. (*a*) Geography of the Bering Strait between Alaska and Russia. The locations of the SAR images used in this case study are indicated by the overlapping squares. (*b*) NOAA 12 AVHRR mapped infrared image of the Bering Sea from the morning of 28 February (1812 UTC). The Alaska Peninsula is located in the bottom right of the image, with the Bering Strait at the top centre. (*c*) ERS-1 SAR image (© ESA 1994) of the Bering Strait from 28 February 1994 (2238 UTC). The Diomede Islands are at the upper right of the image with the Russian coast to the upper left. (*d*) ERS-1 SAR

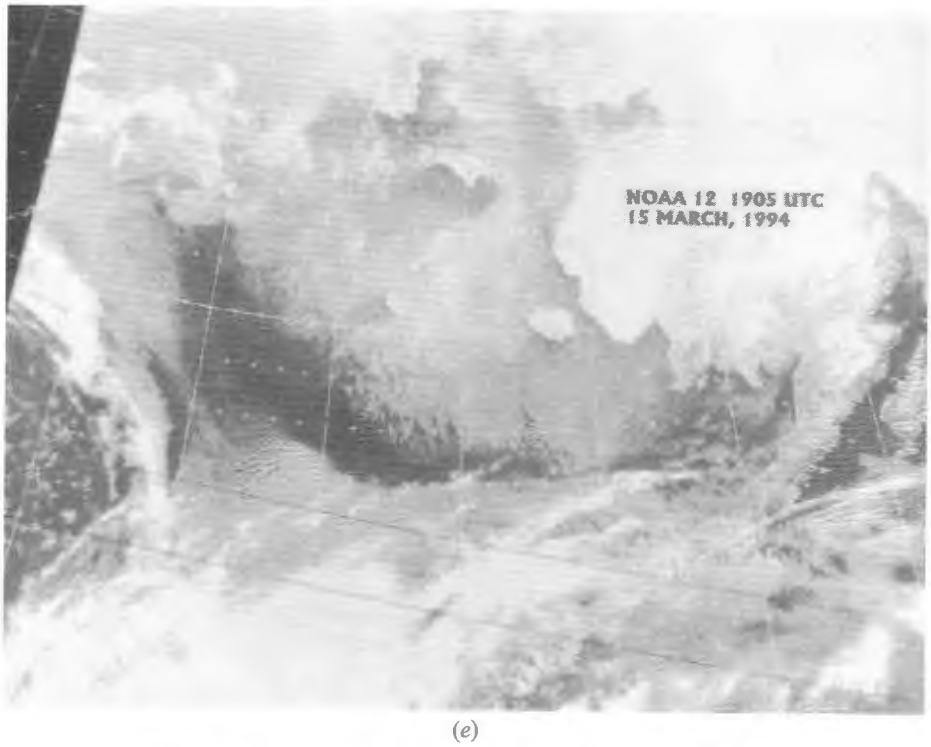

(*e*)

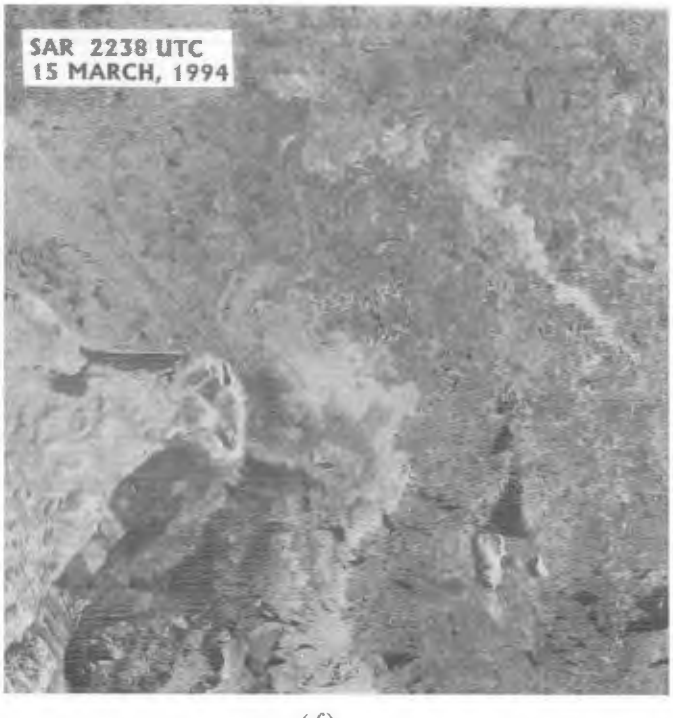

(*f*)

image (© ESA 1994) of the Bering Strait from 3 March 1994 (2238 UTC). The Diomede Islands are at the right centre of the image with the Russian coast to the left. (*e*) NOAA-12 AVHRR mapped infrared image of the Bering Sea from the morning of 15 March 1994 (1905 UTC). The region is the same as for figure 2 (*b*). (*f*) ERS-1 SAR image (© ESA 1994) of the Bering Strait from 15 March 1994 (2238 UTC). The Diomede Islands are at the bottom right of the image with the Russian coast to the left.

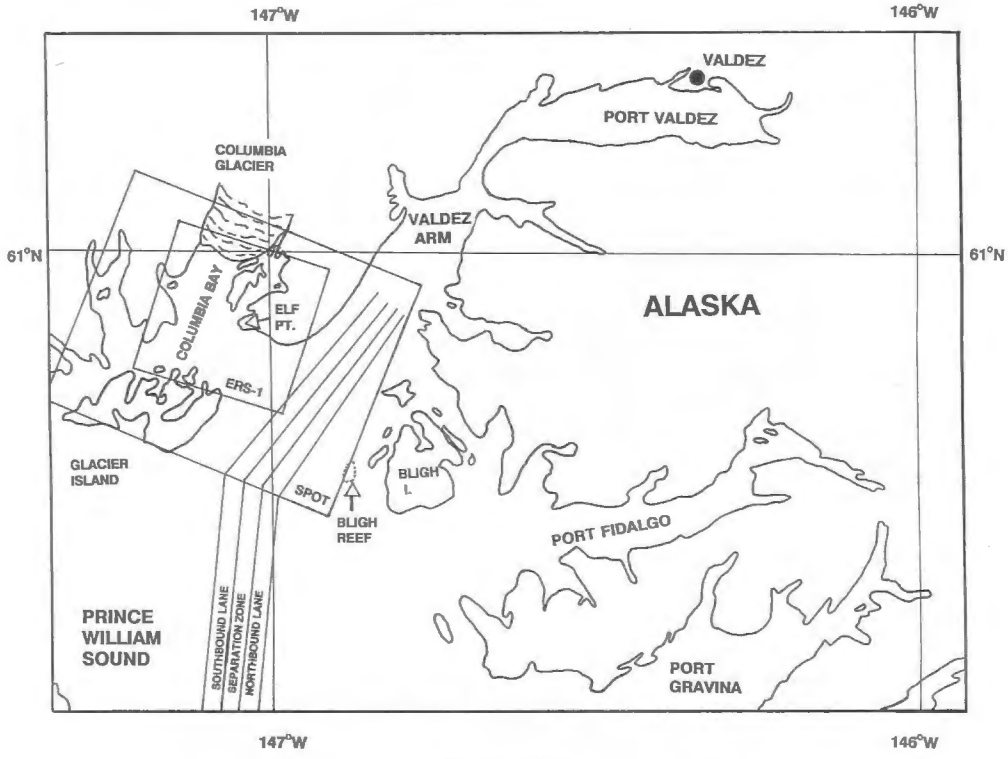

Figure 2 (*a*)

Figure 2 (*b*)

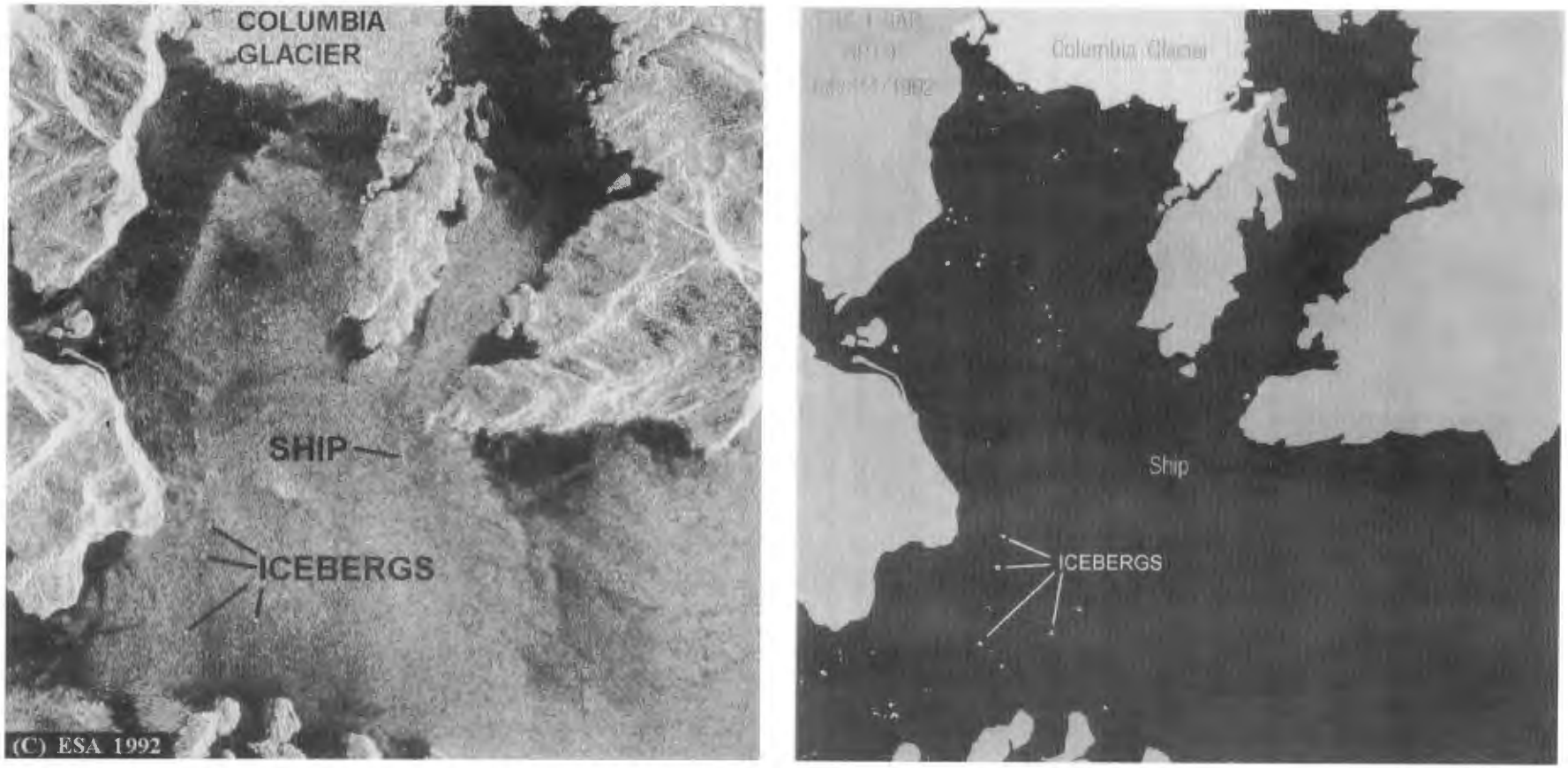

(*c*) (*d*)

Figure 2. (*a*) Map of Prince William Sound, Alaska. The location of images shown in figure 3 (*b*) and 3 (*c*) are indicated by the nested rectangles. (*b*) SPOT image subscene of Columbia Bay, Alaska, 1 July 1992 at 21:19 Z. The resolution of this Multispectral Sensor Channel 1 image (0·50–0·59 μm) is 20 m. The Columbia Glacier is at the top left centre of the image with Columbia Bay to the south. Glacier Island is at the bottom left of the image. Icebergs can clearly be seen drifting out into Valdez Arm in the lower right portion of the image. A ship can be identified by its wake on the western side of Columbia Bay. (*c*) Sub-scene of full-resolution ERS-1 SAR image of Columbia Bay, Alaska, 14 July, 1992, 20:56 Z. (*d*) High-contrast Point Target Discriminator (HPTD) product produced from Figure 3 (*c*) by filtering, thresholding, and contrast enhancement. This product indicates the location of the larger icebergs in Columbia Bay.

Unfortunately, the number of days during the year when Prince William Sound is cloud free is quite limited. The natural question to ask is, are these icebergs imaged in ERS-1 data? If so, the all-weather capability of the SAR could greatly increase the frequency of monitoring opportunities. To answer this question, full-resolution (12·5 m pixels, 30 m resolution) SAR data over Columbia Bay were obtained. Figure 2 (*c*) is a full-resolution 978 by 978 pixel sub-scene sectorized from the full 8192 by 8192 pixel SAR scene of 14 July 1992. The region covered by the sub-scene is indicated in figure 2 (*a*). The Columbia Glacier is at the top left of the image with Columbia Bay to the South. The northern shore of Glacier Island is at the bottom left. A ship can be identified from its wake, just west of Elf Point. Standing out of the enhanced backscatter radar return or sea clutter from the wind-roughened ocean (bright grey speckled regions) within Columbia Bay are numerous highly reflective point targets. Many of these targets have good contrast over the background, especially in darker regions of lower wind speed. Although the SAR image is not time coincident with the SPOT image (it proved impossible to get a cloud-free look from SPOT to coincide with one of the ERS-1 overflights of Prince William Sound), one can infer from the similarity in the patterns of the SAR point targets in Columbia Bay to the pattern of icebergs seen in the SPOT image, that one is able to discern icebergs in the SAR data. Some of the targets, of course, could be buoys or vessels, especially tourist vessels along the face of the glacier. However, the absence of long wakes indicates that most of these point targets are icebergs.

The icebergs in figure 2 (*c*) are visible in the image because their signal is elevated relative to the sea clutter; however, there are probably many small pieces of ice that are not imaged. Most small icebergs, bergy bits (pieces of glacial ice normally 100–300 m^2 in area which extend 1–5 m above sea level), and growlers (pieces $< 100\,m^2$ which extend less than 1 m above sea level) will have signals so similar to the background sea clutter that they cannot be detected (Kirby and Lowry 1979, Rossiter *et al.* 1985). The detectability of an iceberg with a SAR system, as mentioned above, depends on the characteristics of the SAR system, such as radar wavelength, incident angle, signal-to-noise ratio, resolution, and polarization (Larson *et al.* 1978). Just as important for detectability are the physical characteristics of the iceberg and the environment in which it is found. For example, icebergs with steep, vertical sides and those with lots of facets will have greater radar returns (Kirby and Lowry 1979). Other important iceberg physical characteristics are the density and size of included bubbles and ice temperature (Gray and Arsenault 1991). Sea state and the presence of sea ice surrounding the iceberg are some of the important environmental factors influencing detectability.

With all these variables influencing the detectability of icebergs, one cannot tell from a single image how useful the ERS-1 SAR will be for operational monitoring of Columbia Bay. This will depend mainly on the performance characteristics of the SAR, availability of high resolution images, average sea state in the Bay, and iceberg size distribution. This one image, however, confirms that at least the larger (50–70 m diameter as measured from the SPOT image) icebergs in Columbia Bay under favourable conditions of sea state can be identified in 30-m resolution SAR imagery.

To make some first steps toward an iceberg monitoring product, some standard image processing operations were performed on the image in figure 2 (*c*). First, a Lee Filter (Lee 1983) was applied to reduce the speckle, and the display grey scale was altered to increase the contrast of the icebergs. The Lee filter reduces speckle without degrading point targets, by employing local statistics in a small window about each

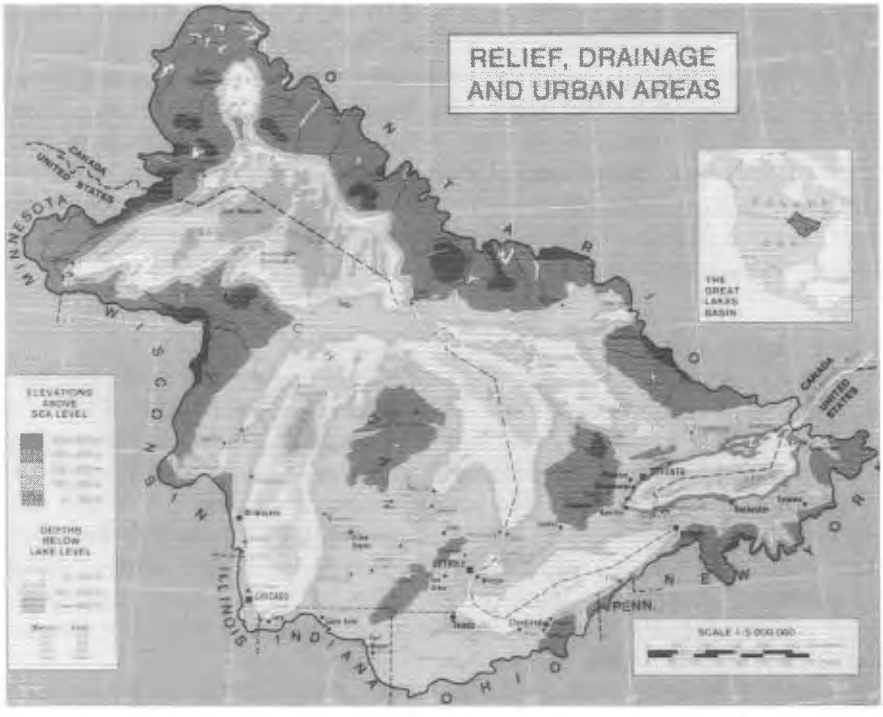

Figure 3. The Great Lakes of North America. From *The Great Lakes Atlas* (USEPA and Environment Canada).

point in the image. Finally, a product (see figure 2(*d*)), which we have called the High-contrast Point Target Discriminator (HPTD) is the result of (1) creating an image of the standard deviation of a 3 by 3 pixel window about each pixel of the Lee-filtered image, which increases the contrast of point targets and edges, (2) thresholding to eliminate pixels with low standard deviation values, and (3) superimposing a land mask produced from the original image. The Columbia Glacier is white, as are the point targets over water (most of which are icebergs). Water is black, land is grey and two small areas near the glacier which are not completely glaciated, but appear to be so on the SAR image, are shown in grey-white. This product shows promise as an iceberg locator.

5. Lake ice case studies in the Great Lakes

Previous studies of the classification and mapping of ice cover on the Great Lakes using Landsat MSS digital data have shown that computer interpretation of satellite digital data is possible for analysis and mapping of Great Lakes ice cover (Leshkevich 1985). However, as in other northern latitude coastal areas during winter months, cloud cover over the Great Lakes region (figure 3) impairs the use of satellite imagery from passive, electro-optical sensors operating in the visible, reflected-infrared, and thermal-infrared for ice cover monitoring and analysis. Even the daily repeat coverage from the AVHRR aboard the NOAA series of weather satellites produces few images (per week) showing enough of the Great Lakes to be of use for operational monitoring during winter months. Although airborne SAR or

side looking airborne radar (SLAR) are used by the U.S. Coast Guard, Canadian Ice Center (Atmospheric Environment Service 1988), and others for operational ice mapping, they are limited in their spatial and temporal coverage, are costly to operate, and are flying weather dependent. Satellite-borne SAR systems, independent of solar illumination and weather conditions, with the promise of routine coverage of the Great Lakes every 3 days in the RADARSAT era, will provide information having application to winter navigation, winter (under ice) ecology, regional climate studies, and shore/near shore erosion and damage as well as long-term ice cover data base development.

5.1. *Great Lakes data set*

A data set for selected areas on the Great Lakes was established covering the period from 18 to 24 February 1993. This data set includes ERS-1 SAR scenes, AVHRR imagery, U.S. Coast Guard SLAR imagery, and airborne reconnaissance data consisting of ice charts, photographs, and video. Based on projected ERS-1 over-pass dates, field data collection was scheduled, with the U.S. Coast Guard providing helicopter flight support. Areas covered on ERS-1 over-pass dates include southern Lake Huron, the St. Clair River, the Detroit River, and western Lake Erie on 18 February; central and eastern Lake Erie on 19 February; western Lake Superior and the Apostle Islands on 23 February; and the Straits of Mackinac, Whitefish Bay, and St. Marys River on 24 February.

Oblique, colour aerial photographs and video along with ice charts and locational (Loran) data were obtained over the study areas from altitudes ranging from approximately 200 to 400 m. Ice thickness was obtained for two of the areas (southern Lake Huron and Straits of Mackinac) from Coast Guard ice breaking vessels. ERS-1 data from the Gatineau readout station in Canada were received via a link between the U.S. and Canadian Ice Centres, and mapped to a polar stereographic projection on the NIC SAR Workstation. Five scenes covering the study areas, each nominally 100 km square with 50 m resolution, were downloaded to the Great Lakes Environmental Research Laboratory (GLERL). This data set, along with meteorological data from selected ground stations, was used in the analysis. Preliminary analysis of two of the scenes (Straits of Mackinac and western Lake Superior) are described here. For additional analysis see Leshkevich *et al.* (1994).

5.2. *Methods*

The SAR images were displayed and analysed using commercial and government-developed image processing software. For each of the two scenes, a 512 by 512 pixel sub-scene was abstracted and used for the analysis. Since the SAR data are mapped or geocoded, observed ice types and features can be located and identified in the imagery using Loran coordinates recorded in flight. It should be noted that SAR scenes received by the Gatineau readout station were not calibrated. Thus, in this study, identification and association of dB (decibel) values with individual ice types was not possible. This was not a limiting factor in this study, but would be for any multi-temporal analysis. However, software has been developed to do a retrospective calibration (Manore, personal communication, 1993) and it is planned to use this capability in future analysis and for images obtained during the 1994 winter season for the demonstration phase of this study.

Two image processing techniques were used in this initial analysis. The first was a supervised, level slicing classification (Lillesand and Kiefer 1979) based on a comparison of brightness or digital values in the SAR scene representing known ice types as identified in the ground data. Using the ground data, ice types, open water, and land were identified in the displayed SAR image and a representative 'training set', consisting of a range of digital values, for each type was extracted. A colour was assigned to each ice type (range of values) using the convention of dark colours (blue, green, etc.) for lower values and bright colours (red, magenta, etc.) for higher values. The colour assigned to each range was applied to the entire sub-scene producing a colour-coded classified image. Most of each of the two sub-scenes was classified with six to seven representative ranges. With iterative testing, this took approximately 2 h per scene. For operational use, a more objective, less time consuming method of analysis is needed. The second method used to analyse the SAR images was an unsupervised, statistical technique called K-means or KCLUS (Lillesand and Kiefer 1979). This clustering algorithm produces spectral classes based on natural groupings of the image values. After determining six spectrally separable classes, their identity was defined based on the field data and results of the supervised classification.

5.3. *Results and discussion*

It was found that the patterns were very similar between the two techniques and that for most classes (especially in the Straits of Mackinac sub-scene), the mean value for each cluster fell within or bordered the range of values determined in the first technique using the field data. However, further research needs to be conducted on the repeatability of the techniques in scenes imaged at different times during the season, under different temperature (melt) and wind conditions.

The original colour-coded classified images have been annotated to better illustrate features and ice types in the image. Ice types referred to in this report are described in the nomenclature set forth in the 'Ice Glossary' (Lake Survey Center 1971).

5.3.1. *Straits of Mackinac*

Figure 4(*a*) is an ERS-1 SAR image of the Straits of Mackinac, connecting Lakes Michigan and Huron, on 24 February 1993. Prominent features in the scene include the bright, north – south trending linear feature (Mackinac Bridge) connecting the lower and upper peninsulas of Michigan. The bright east–west trending line perpendicular to the bridge is a shipping lane in the ice which turns to the north-east just east of the bridge. Figure 4(*b*) is an aerial photograph (looking eastward) showing the bridge, the shipping lane, and black ice (WMO—thin first-year ice/white ice) with some snow wind rows on the surface. There are no areas of open water in the sub-scene except, perhaps in the shipping lane and some open cracks. Midday temperatures averaged −15° C. The shipping lane shows a bright return due to the high backscatter from the rough-textured 'brash ice' (broken pieces) in the track. Bright returns from along the shorelines are also caused by the ice broken by wind and wave action previously being pushed and piled on or near shore. Darker tones in the sub-scene are caused by low backscatter from areas of relatively smooth, black ice where the radar pulse either penetrates or is reflected obliquely from the ice surface (Shuchman *et al.* 1991). Ice, west of the bridge and south of the shipping lane is cracked and ridged and shows up as bright returns in the image. Ice, east of the

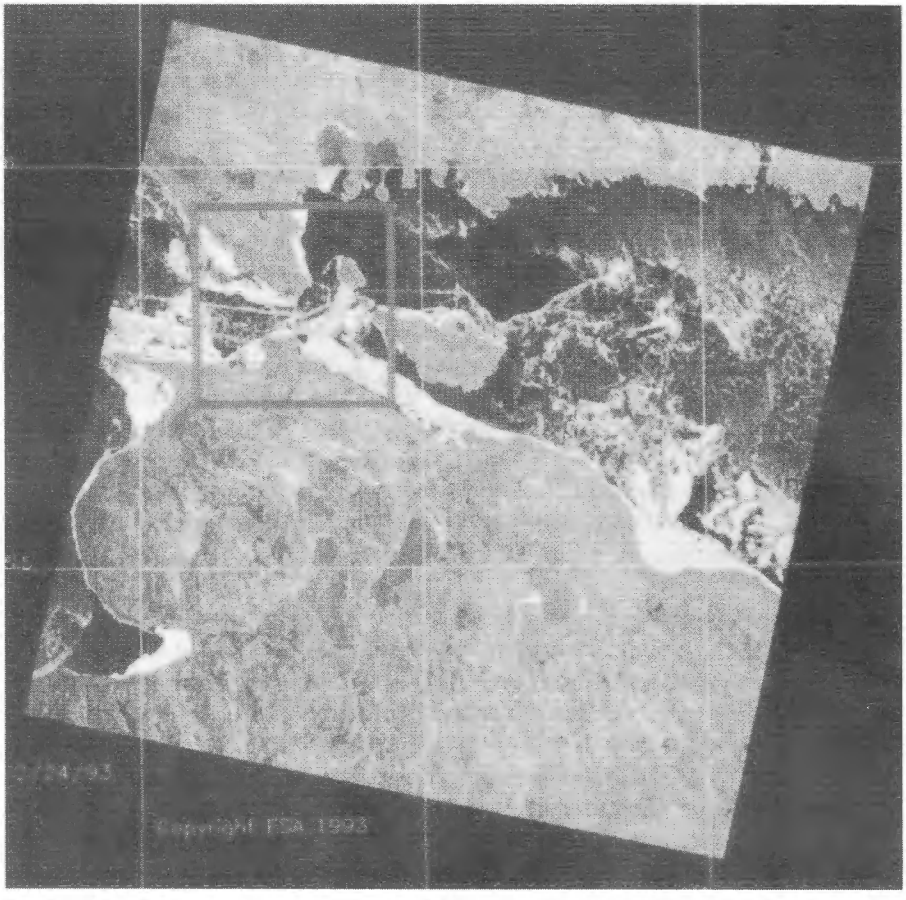

(*a*)

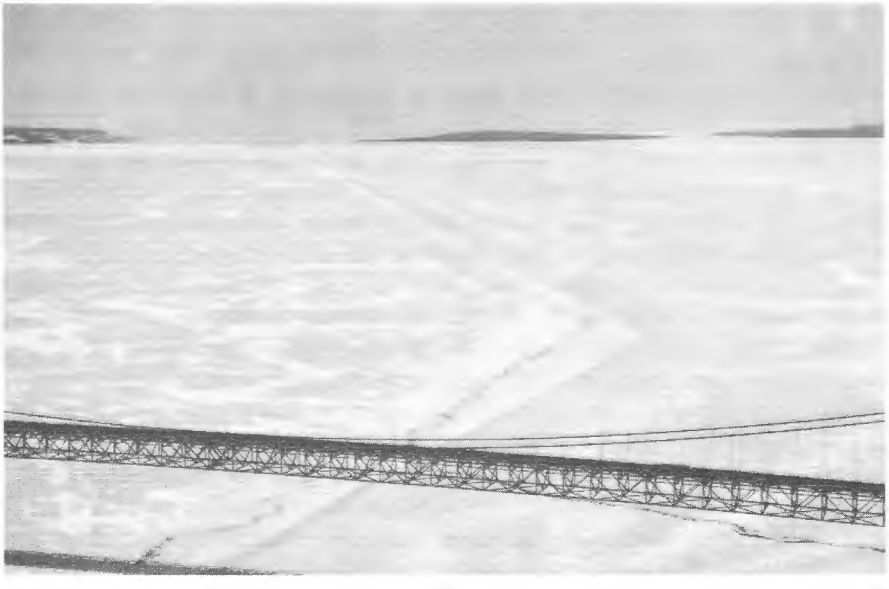

(*b*)

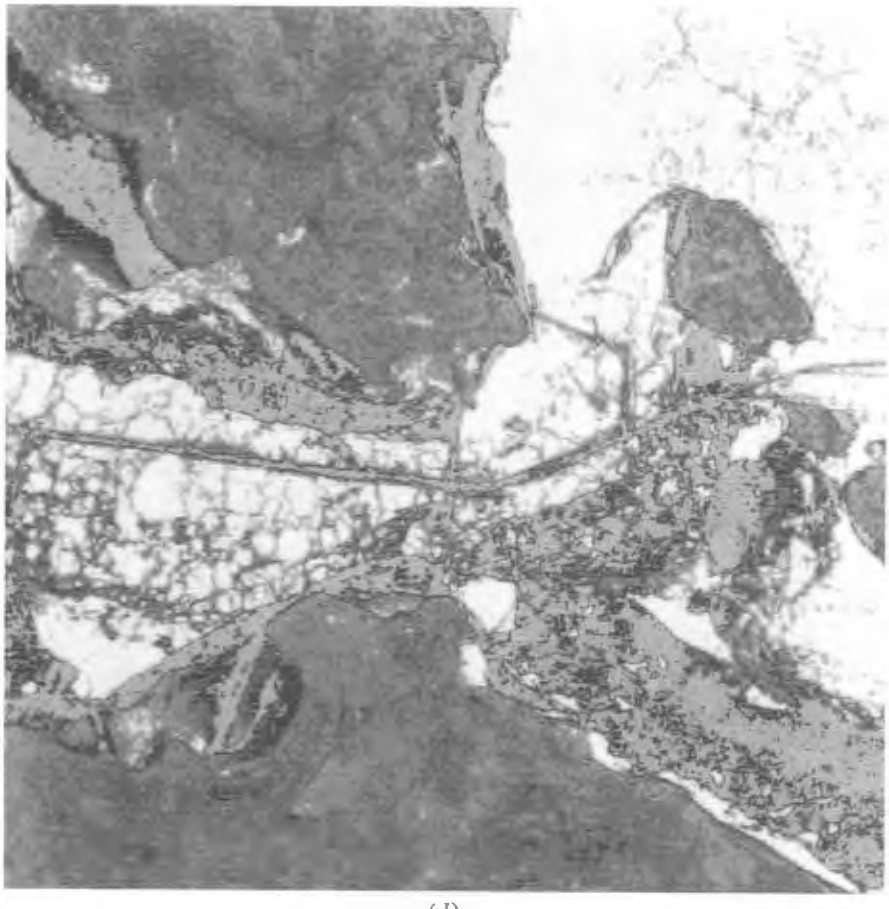

(*d*)

Figure 4. (*a*) ERS-1 SAR image of the Straits of Mackinac on 24 February 1993 study area within box. (*b*) Aerial photograph (looking east) showing Mackinac Bridge, ship track, and ice cover. (*c*) Annotated image showing results of supervised, level slicing classification. (*d*) Image showing results of unsupervised clustering (*K*-means) classification.

bridge and north of the ship track has few cracks and ridges and is 38–40 cm thick as reported by a Coast Guard ice breaker. Land has a characteristic return (tone and texture) based on terrain and topographical features. Two frozen inland lakes can be seen in the SAR image (outside the sub-scene) at about 45·5° N and 84·5° W. At that location is Mullet Lake and just to the west of it, Burt Lake. The tone and texture of these lakes is noticeably different than that from ice in the study area. Although returns from the bottom of shallow Arctic lakes have been observed (Mellor 1994), Mullet and Burt Lakes are both relatively deep and not frozen to the bottom. The backscatter could be caused by (1) a layer of 'snow ice' or 'slush ice' that usually forms on these inland lakes by February or (2) moisture-laden snow cover caused by rainfall.

Land and five ice types were found to classify most of the sub-scene. Figure 4(*c*) illustrates the results of the supervised, level slicing classification. Figure 4(*d*)

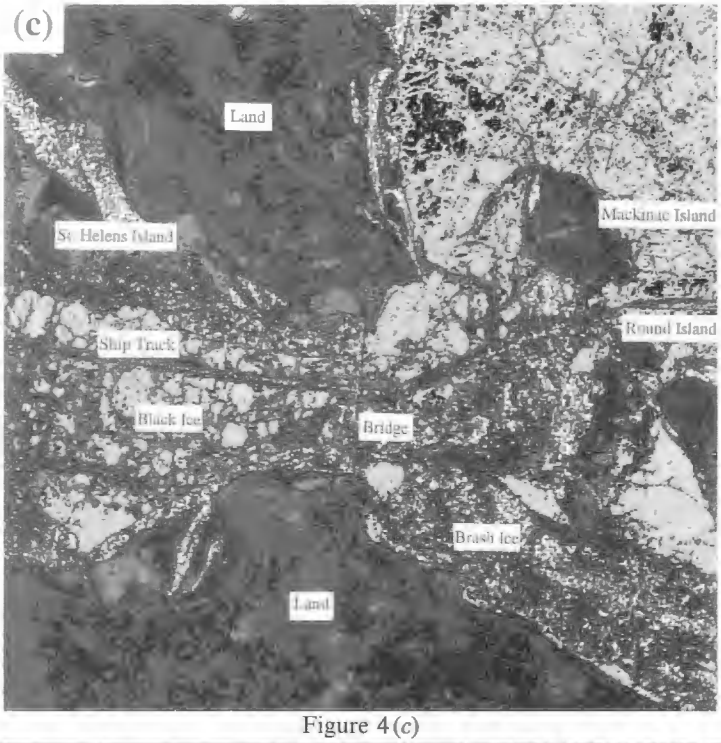

Figure 4(*c*)

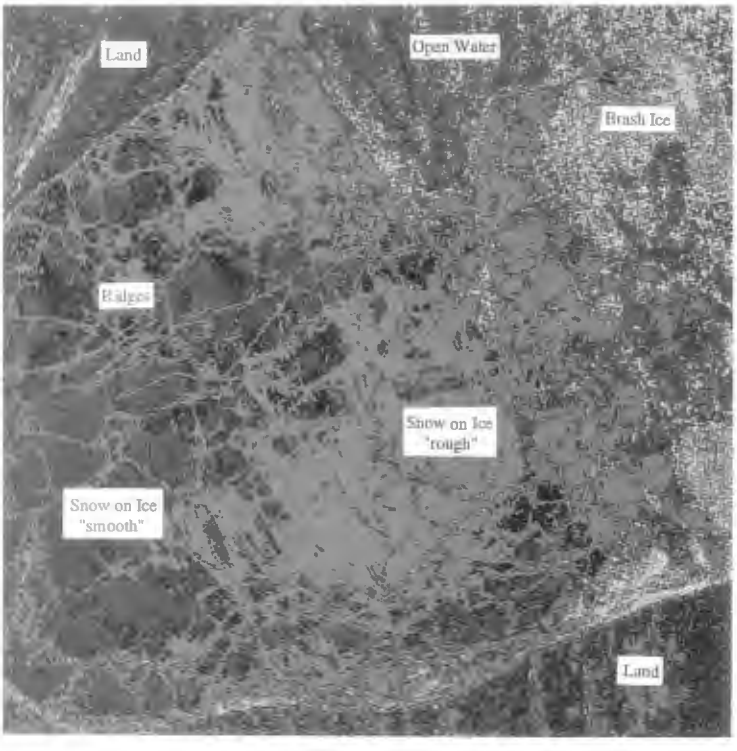

Figure 5(*c*)

illustrates the results of the unsupervised, statistical (*K*-means) clustering algorithm. The patterns are definitely similar to the supervised technique and mean brightness values for the clusters were within or bordered the range of digital values picked as 'training sets' for the supervised technique. It would be fairly easy to assign ice types to the clusters based on field observations.

5.3.2. *Western Lake Superior*

Other than in bays and harbours, ice cover on Lake Superior usually forms first in the shallower western basin and grows eastward. After the spring 'breakup', ice usually retreats westward. The area around the Apostle Islands and the western end of the lake are usually the last areas to become ice free. As major exporters of wheat, western coal, and taconite, Two Harbors and Duluth (Minnesota) at the western end of the lake are affected by the duration and severity of the ice cover. Figure 5 (*a*) is an ERS-1 SAR image of the western end of Lake Superior on 23 February 1993. The study area (sub-scene) is enclosed by the box. Figure 5 (*b*) is an aerial photograph (looking north) showing cracks and pressure ridges in the ice cover. The surface, covered by wind blown snow, has a low backscatter return (dark) in the SAR image. This is probably the result of the relatively smooth lake (black) ice surface beneath the snow. As for the Straits of the Mackinaw study area, aerial photos, ice charts and other ground data were used to pick training areas for which digital values were extracted. Using the level slicing technique, the sub-scene was then colour coded using the same colour scheme employed previously (figure 5 (*c*)). Land and areas of open water, 'rough' and 'smooth' snow-covered ice (similar in thickness to thin first-year ice), ridges, and brash ice were identified. The brighter returns from the 'rough' snow-covered ice could be due to deformation of the ice sheet by wind and wave action which could have contributed to the formation of a porous snow ice or slush ice layer. The bright return from the lake surface to the northeast of the study area (figure 5 (*a*)) is the backscatter from open water. This open water extends into the study area (top centre) and although the backscatter is less here than from the larger area of open water to the northeast, signal values are actually similar to those from some land areas. Backscatter is probably lower here due to the relatively small size of the open water area which is enclosed on three sides by land or ice cover and thus less susceptible to wind action (figure 5 (*a*)). The bright areas along the northeast, south, and southeast of the study area are caused by high backscatter from ridged or rafted ice along the shore or brash ice along the ice edge.

Using only backscatter (single channel, single polarization), it was found that the signal from open water was close to that from some land areas and that one ice type produced signal values close to those in some areas of open water. In an effort to evaluate the use of another dimension in addition to backscatter brightness values, a texture analysis algorithm was used to derive 'texture' or 'spatial frequency' (Lillesand and Kiefer 1979) in the study area (figure 5 (*d*)). The use of this spatial dimension in addition to the spectral dimension in a multivariate classification procedure could improve the classification and interpretation of ice cover in the SAR images.

6. Demonstration phase

The case studies accomplished to date have been valuable in; (1) determining which possible applications of SAR data have value for coastal environmental

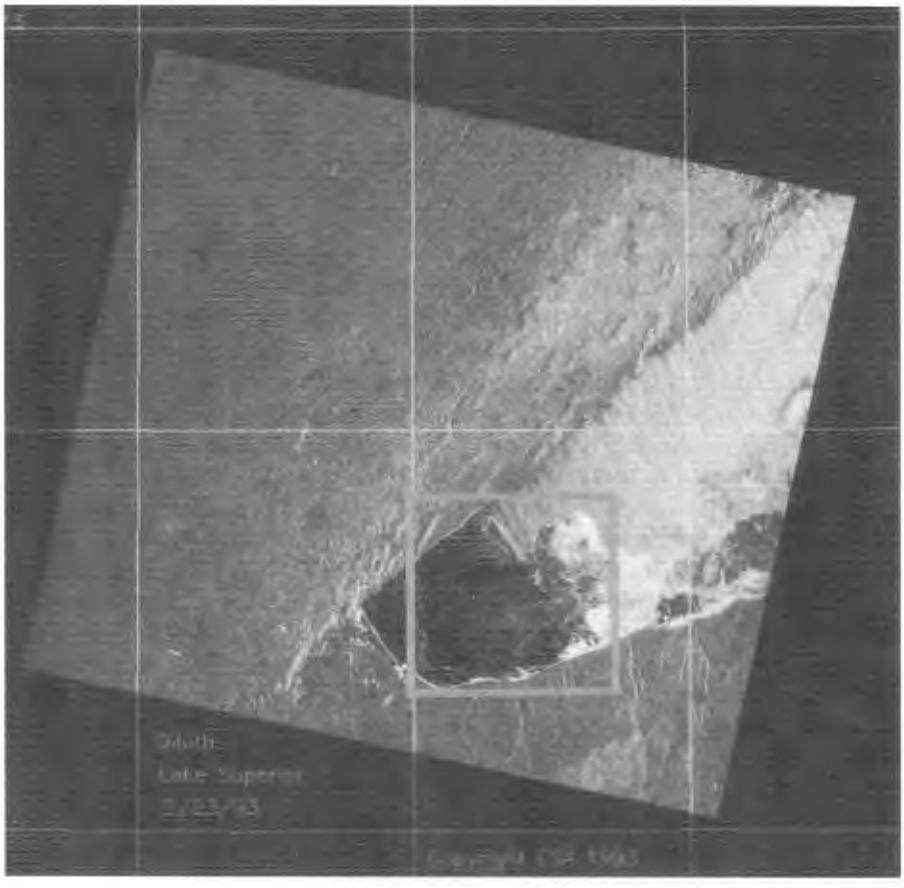

(*a*)

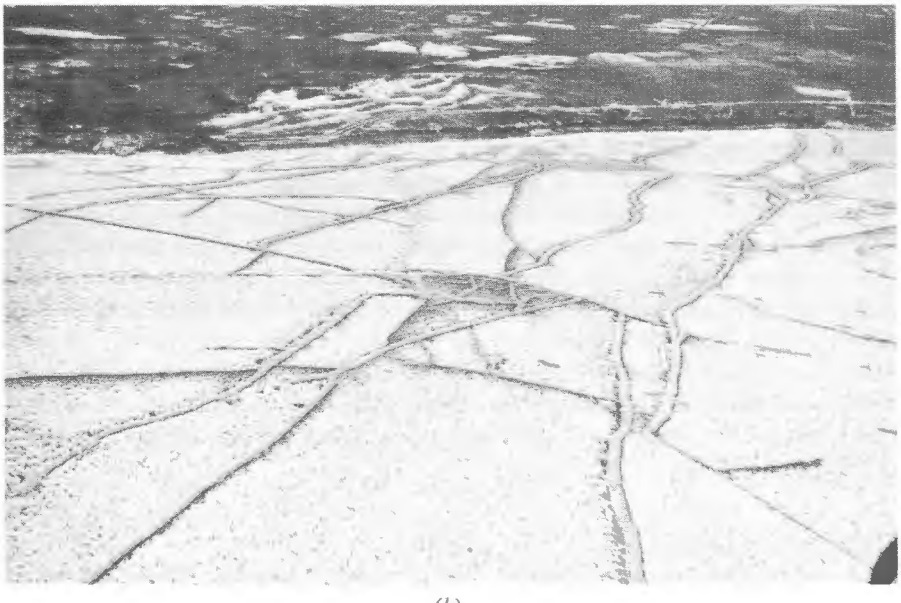

(*b*)

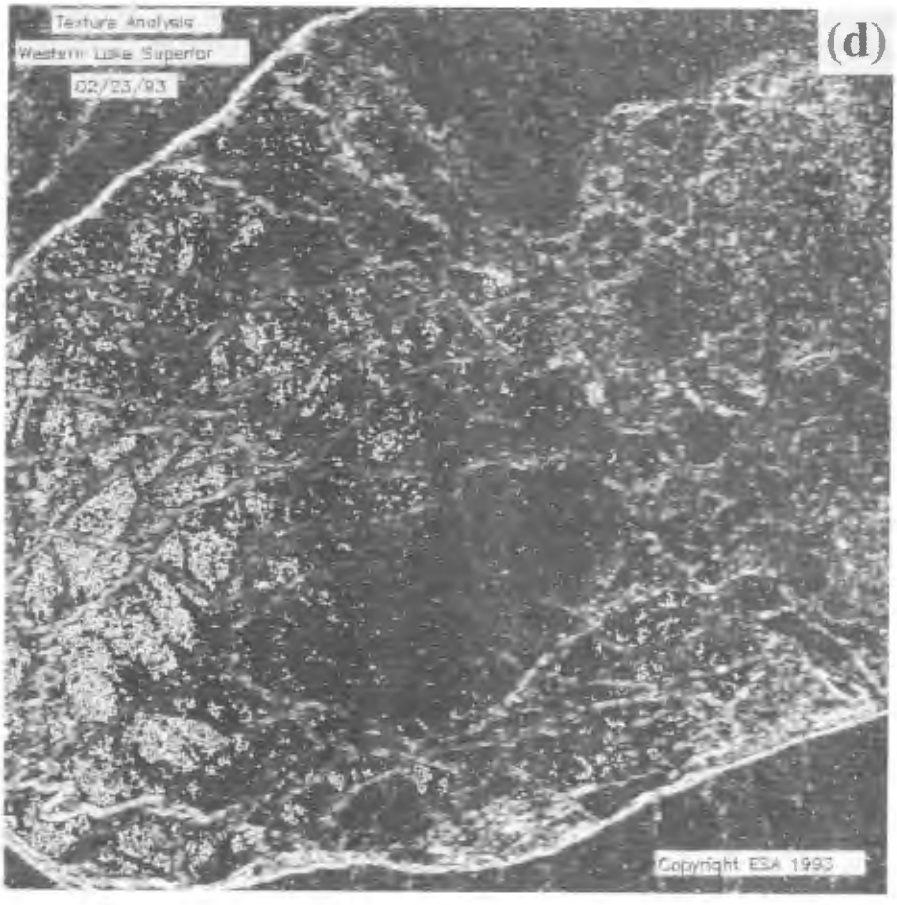

(*d*)

Figure 5. (*a*) ERS-1 SAR image of western Lake Superior on 23 February 1993 study area within box. (*b*) Aerial photograph (looking north toward shore) showing cracks and ridges in the ice cover. The surface is covered by wind blown snow. (*c*) Annotated image showing results of supervised, level slicing classification. (*d*) Image showing results of texture analysis. The brighter areas have the 'rougher textures' such as the ice piled up along the shoreline, the area of brash in the northeast portion of the sub-scene, and the roughened, wind-blown, snow-covered surfaces.

management activities, and (2) giving the participants needed experience in techniques useful in working with SAR data. The next phase of this effort began in January 1994 with the initiation of an applications demonstration in the Great Lakes. Using data from the 3-day repeat orbit of ERS-1, images were obtained for Lakes Michigan, Superior, and Erie on a routine basis and evaluated for use in Greak Lakes ice reconnaissance and forecasting. Sample images were supplied to the U.S. Coast Guard and the National Weather Service for evaluation in operational use during the demonstration. These data are now being studied to see if the classification procedures developed for the case studies can be applied consistently over the ice season. Retrospective calibration of the 1994 SAR data is planned.

Based on additional ground data collected, look-up tables will be developed for evaluation in ice cover classification from scene to scene and results compared to methods described in this paper. Demonstrations of coastal ice analysis and forecasting and river ice-jam monitoring in Alaska are also under way.

7. Summary

The NOAA National Environmental Satellite, Data, and Information Service, together with two NOAA CoastWatch Regional Sites at the National Weather Service Anchorage Forecast Office in Alaska and the Great Lakes Environmental Research Laboratory in Ann Arbor, Michigan are participating in an applications demonstration of the utility of SAR data to coastal management and monitoring activities. In order to develop the ability to process and interpret SAR data, case studies were accomplished in which SAR data were collected and compared to correlative data such as AVHRR thermal and visible data as well as aerial photos and video. In coastal Alaskan waters it was found that the high resolution and all-weather viewing capability of SAR provided monitoring information unobtainable from other data sources. An analysis of full resolution SAR data of Columbia Bay indicates that at least some of the icebergs calved from the Columbia Glacier are imaged in these data. Image processing techniques can be used to highlight the icebergs. For the Great Lakes, two image processing techniques were used to interpret and analyse ice types in ERS-1 SAR images of two important areas. Preliminary analysis indicates that different ice types in the ice cover can be identified, classified, and mapped. In addition, wind has a strong influence on the backscatter from open water, and new (dry) snow is essentially transparent at the SAR C-Band wavelength, phenomena that has been documented by others as well. The two techniques produced relatively similar results, which may be further improved upon by using texture as an added dimension in a multivariate classification procedure.

Acknowledgments

SAR data for this demonstration were provided by the European Space Agency within the framework of the Programme for International Polar Oceans Research (ERS-1 Experiment ID: USPW1102, PIPOR proposal PI/BCB12). Funding to support the demonstration was provided by the NOAA Coastal Ocean Program. The imagery used in this applications demonstration could not have been obtained and processed without the efforts of many at the Alaska SAR Facility (especially Greta Reynolds), the Ice Center Environment Canada (especially Robert Tessier and Terry Mullane), the Canadian Centre for Remote Sensing (especially Bonnie Harris), the National Ice Center (especially Selina Nauman, Mark Dunn, Jim Nolan, and Cheryl Bertoia), and the Naval Research Laboratory (especially Florence Fetterer and Conrad Johnson). Gary Wohl of the National Weather Service gave valuable advice in the interpretation of the Columbia Bay imagery. Our appreciation and thanks go to the U.S. Coast Guard, Ninth District for providing the helicopter flight support essential to the success of the Greak Lakes demonstration. GLERL Contribution Number 882.

References

Atmospheric Environment Service, 1988, *Ice Services in Canada* (Ottawa: Environment Canada, Atmospheric Environment Service, Ice Branch), 10 pp.

BATTRICK, B., (ed.), 1993, *ERS User Handbook*, ESA Sp-1148 (Noordwijk: ESA Publications Division), 129 pp.

CELONE, P., and SMITH, R., 1992, Satellite imagery for environmental monitoring and management: NOAA's CoastWatch is administration's contribution to coastal resource management for the 1990s. *Sea Technology*, **33,** 10–23.

GRAY, A., and ARSENAULT, L., 1991, Delayed reflections in L-Band synthetic aperture radar imagery of icebergs. *I.E.E.E. Transactions on Geoscience and Remote Sensing*, **29,** 284–291.

HALL, D. K., and MARTINEC, J., 1985, *Remote Sensing of Ice and Snow* (New York: Chapman and Hall).

KIRBY, M., and LOWRY, R., 1979, Iceberg detectability problems using SAR and SLAR systems. *Satellite Hydrology, Proceedings of the Fifth Annual William T. Pecora Memorial Symposium on Remote Sensing, Sioux Falls, South Dakota, 10–15 June 1979* (Minneapolis: American Water Resources Association), pp. 200–212.

Lake Survey Center, 1971, *Ice Glossary*, HO 75-602 (Detroit: U.S. Department of Commerce, National Oceanic and Atmospheric Administration, National Ocean Survey, Lake Survey Center), 9 pp.

LARSON, R., SHUCHMAN, R., and RAWSON, R., 1978, The use of SAR systems for iceberg detection and characterization. *Proceedings of the Twelfth International Symposium on Remote Sensing of Environment, Vol. II, Ann Arbor, MI, 20–26 April, 1978* (Ann Arbor, MI: Environmental Research Institute of Michigan), pp. 1127–1147.

LEE, JON-SEN., 1983, A simple speckle smoothing algorithm for synthetic aperture radar images. *I.E.E.E. Transactions on Systems, Man and Cybernetics*, **13,** 85–89.

LESHKEVICH, G., 1985, Machine classification of freshwater ice types from Landsat-1 digital data using ice albedos as training sets. *Remote Sensing of Environment*, **17,** 251–263.

LESHKEVICH, G., PICHEL, W., and CLEMENTE-COLON, P., 1994, Great Lakes SAR ice research applications demonstration. *Space at the Service of Our Environment, Proceedings of the Second ERS-1 Symposium, Hamburg, Germany, 11–14 October 1993*, ESA Sp-361, vol. 2 (Paris: European Space Agency), pp. 675–679.

LESHKEVICH, G., SCHWAB, D., and MUHR, G., 1993, Satellite environmental monitoring of the Great Lakes: a review of NOAA's Great Lakes CoastWatch program. *Photogrammetric Engineering & Remote Sensing*, **59,** 371–379.

LEWIS, E. O., CURRIE, B. W., and HAYKIN, S., 1987, *Detection and Classification of Ice* (Letchworth, Research Studies Press Ltd.)

LILLESAND, T. M., and KIEFER, R. W., 1979, *Remote Sensing and Image Interpretation* (New York: John Wiley & Sons).

MELLOR, J. C., 1994, ERS-1 SAR use to determine lake depths in Arctic and subarctic regions. *Space at the Service of Our Environment, Proceedings of the Second ERS-1 Symposium, Hamburg, Germany 11–14 October 1993*, ESA Sp-361, vol. 2 (Paris: European Space Agency), pp. 1141–1146.

OLMSTED, C., 1993, Alaska SAR facility scientific SAR user's guide. Geophysical Institute, University of Alaska Fairbanks, ASF-SD-003, 53 pp.

PICHEL, W., WEAKS, M., SAPPER, J., TADEPALLI, K., JANDHYALA, A., and KETINENI, S., 1991, Satellite mapped imagery for CoastWatch. *Proceedings of 7th Symposium on Coastal & Ocean Management ASCE/Long Beach, CA, 8–12 July 1991* (New York: American Society of Civil Engineers), pp. 2531–2545.

PICHEL, W., CLEMENTE-COLON, P., HUFFORD, G., LESHKEVICH, G., WOHL, G., KNISKERN, F., SAPPER, J., and CAREY, R., 1994, CoastWatch SAR applications demonstration development phase. *Space at the Service of our Environment, Proceedings of the Second ERS-1 Symposium, Hamburg, Germany, 11–14 October 1993*, ESA SP-361, vol. 2 (Paris: European Space Agency), pp. 669–674.

ROSSITER, J., ARSENAULT, L., GUY, E., LAPP, D., WEDLER, E., MERCER, B., MCLAREN, E., and DEMPSEY, J., 1985, Assessment of airborne imaging radars for the detection of icebergs. Environmental Studies Revolving Funds, Report No. 016, Ottawa, 338 p.

SHUCHMAN, R., WACKERMAN, C., and SUTHERLAND, L., (eds.), 1991, *The Use of Synthetic Aperture Radar to Map the Polar Oceans* (Ann Arbor, MI: ERIM).